

11051
86854
p. 23

NASA Technical Memorandum 105387

Evaluation of MHOST Analysis Capabilities for a Plate Element

Ho-Jun Lee
National Aeronautics and Space Administration
Lewis Research Center
Cleveland, Ohio

Galib H. Abumeri and Helen C. Brown
Sverdrup Technology, Inc.
Lewis Research Center Group
Brook Park, Ohio

February 1992



(NASA-TM-105387) EVALUATION OF MHOST
ANALYSIS CAPABILITIES FOR A PLATE ELEMENT
(NASA) 23 p

CSSL 20K

N92-23196

Unclas
0086854

G3/39



EVALUATION OF MHOST ANALYSIS CAPABILITIES FOR A PLATE ELEMENT

Ho-Jun Lee
National Aeronautics and Space Administration
Lewis Research Center
Cleveland, Ohio 44135

and

Galib H. Abumeri and Helen C. Brown
Sverdrup Technology, Inc.
Lewis Research Center Group
Brook Park, Ohio 44142

SUMMARY

Results of the evaluation of the static, buckling, and free vibration analyses capabilities of MHOST for the plate element are presented. Two large scale, general purpose finite element codes (MARC and MSC/NASTRAN) are used to validate MHOST. Comparisons of MHOST results with those from MARC and MSC/NASTRAN show good agreement and indicate that MHOST can be used with confidence to perform the aforementioned analyses using the plate element.

INTRODUCTION

MHOST (ref. 1) is a finite element code designed to perform nonlinear analysis of turbine engine hot section components. It employs a mixed iterative finite element technology, as well as an option for a standard displacement method, designed specifically for inelastic three-dimensional solid and structural analysis. The MHOST element library contains 13 two- and three-dimensional elements that can be used to solve various engineering problems. Typical elements include the beam, plate, brick, plane stress, plane strain, and axisymmetric elements. MHOST is capable of handling all types of boundary conditions, most kinds of loadings (i.e., concentrated, distributed, pressure, temperature, transient, etc.), isotropic and anisotropic materials, elastic and inelastic analyses, as well as eigenvalue extraction for buckling and vibration analyses.

MHOST was developed at MARC Research Corporation under a contract for NASA Lewis Research Center. As well as being used to perform finite element analysis independently, MHOST has also been integrated with different in-house micromechanics codes to produce several stand alone structural analysis computer programs. Among these codes are (1) CODSTRAN (ref. 2) which is used to simulate progressive fracture in polymer matrix composites, (2) HITCAN (ref. 3) for performing structural analysis of metal matrix composites, and (3) STAHYC (ref. 4) to optimally design composite structures for applications to hypersonic propulsion ducts. Due to the wide in-house use of MHOST, the various analysis capabilities for the different elements must be evaluated to use the code with confidence. In this study, two large scale general purpose finite element codes, MSC/NASTRAN (ref. 5) and MARC (ref. 6), as well as available theoretical results, are used to validate MHOST for the plate element for the static, buckling, and vibration analyses. The purpose of this work is to check the different analysis capabilities of MHOST in comparison to other existing finite element codes. As such,

issues regarding element formulation, convergence, different aspect ratios, etc are outside the scope of this work and will not be addressed.

FINITE ELEMENT MODEL

The finite element model used throughout this study is a 5.0 in. square plate with a thickness of 0.2 in. as shown in figure 1(a). The model consists of 121 nodes and 100 elements as illustrated in figures 1(b) and (c). The element used is a four noded isoparametric membrane-bending plate element, element 75 for MHOST and MARC, and CQUAD4 for MSC/NASTRAN. The standard displacement option is used in MHOST, since MARC and MSC/NASTRAN are both based on displacement formulations.

A total of 19 cases were examined for both isotropic and anisotropic materials, with a variety of boundary conditions for three analyses (static, buckling, and vibration). The material properties of aluminum were chosen for the isotropic analysis, while the anisotropic material properties were chosen from the composite properties of a $[0/90]_s$ SiC/Ti-15-3 metal matrix composite (fig. 2). For the purposes of this study, the temperature dependent nonlinear material behavior of SiC/Ti-15-3 is not considered.

It should be noted that the choice of a square plate and a $[0/90]_s$ laminate for the anisotropic material properties for the comparisons in this study may not result in the best test cases. The square plate was chosen in order to have a reference for later studies on larger aspect ratios, while the choice for the $[0/90]_s$ laminate was due to the ready availability of material properties.

STATIC ANALYSIS

Twelve cases were studied in the static analysis for a variety of boundary conditions (table I). Half the cases utilized isotropic material properties, while the other half used anisotropic material properties. Loading conditions included concentrated forces, distributed loads, uniform heating, temperature gradients through the thickness, and combinations of heating with either a concentrated force or distributed load. For the isotropic cases, displacements and stresses at the center of the plate are presented, while for the anisotropic cases, displacements, stress resultants, and moment resultants at the center of the plate are presented. For some of the isotropic cases, theoretical solutions are listed when available instead of MARC solutions.

The first two isotropic cases have all four edges simply supported. The first case has a concentrated force applied at the center (fig. 3), while the second case has a distributed load over the top surface (fig. 4). The next two cases involve uniform heating (fig. 5) and a temperature gradient through the thickness (fig. 6) with all four edges restrained. The two final cases for the isotropic material properties involve a combination of uniform heating and a distributed load with all edges pinned (fig. 7) and a temperature gradient through the thickness and an edge load with all edges restrained (fig. 8).

Comparisons of the displacements and stresses predicted by the three codes for the isotropic static analysis shows good agreement between the three codes. Generally, errors in displacements and stresses between both MHOST-MARC and MHOST-MSC/NASTRAN are less than 3.0 percent, with many of the results being almost identical. The one exception is for the

problem in figure 3 (a concentrated load applied at the center of a simply supported plate) which has differences in stresses of 13.4 percent between MHOST and MSC/NASTRAN (the reason for these large differences will be discussed in a subsequent section).

The next set of six cases involves anisotropic material properties. The first case has a concentrated force applied at the center of a plate with three edges simply supported and one edge free (fig. 9). The second case has all four edges simply supported with a distributed load on the top surface (fig. 10). Figure 11 models a uniform heating of a plate restrained on all four edges, while figure 12 shows a temperature gradient through the thickness for a plate with three simply supported edges and one edge free. The fifth and sixth cases both have three edges simply supported and one free. The fifth case combines a concentrated force at the center with a uniform heating (fig. 13). The sixth case has the same concentrated force along with a temperature gradient through the thickness (fig. 14).

Comparisons of the displacements and stress resultants for all six anisotropic cases again show excellent agreement, with errors of less than 2.0 percent for both MHOST-MARC and MHOST-MSC/NASTRAN. Generally, larger differences exist in predictions of the moment resultants between the three codes. MHOST-MARC results show differences of less than 4.0 percent, while MHOST-MSC/NASTRAN errors are less than 13.0 percent.

BUCKLING ANALYSIS

The buckling analysis is conducted on three cases (table II) under a compressive edge load. The critical buckling load is determined for each case. The first case has two edges clamped and the other two edges simply supported for an isotropic material. Results are presented in figure 15. The second case has the same configuration as the first case with the addition of a uniform heating effect (fig. 16). As expected, the addition of a thermal load dramatically reduces the critical buckling load. The third case has all four edges simply supported for an anisotropic material (fig. 17). For all three buckling cases, differences between MHOST-MARC and MHOST-MSC/NASTRAN predicted critical buckling loads are less than 6.0 percent.

FREE VIBRATION ANALYSIS

In the free vibration analysis four cases are examined (table III) and the first three natural frequencies predicted. The first two cases, figures 18 and 19, are for an isotropic material. The first case has all four edges clamped, while the second case has two edges clamped and the other two simply supported. The third and fourth cases use anisotropic material properties and have the same boundary conditions as the two isotropic cases (figs. 20 and 21).

Comparisons between MHOST-MARC and MHOST-MSC/NASTRAN results for the free vibration analyses show that for both isotropic and anisotropic materials, there is a reduction in the natural frequencies for the two edges clamped-two edges simply supported case from the four edges clamped case. Generally, predictions for the first natural frequency are more accurate than the second and third frequencies and better agreement is obtained between MHOST and MARC, with a maximum error of less than 1.2 percent, than between MHOST and MSC/NASTRAN, which has a maximum error of 5.2 percent.

DISCUSSION

Typically, differences between MHOST and MARC results are expected to be less than the corresponding MHOST and MSC/NASTRAN results. This behavior is a consequence of the similarities in the displacement based formulations of MHOST and MARC and is most readily observed in the static anisotropic material property analysis. For the set of six cases involved (figs. 9 to 15), moment resultant predictions between MHOST-MARC have differences of less than 4.0 percent, while MHOST-MSC/NASTRAN differences are less than 13.0 percent.

A consequence of all three codes making use of a displacement based formulation is that the best agreement is expected for predictions of displacement. Since stresses and moments are derived from the displacements, errors for stresses should increase, and errors for moments should become even larger. This implies that the most credible comparison lies in the displacement predictions. Examining the 12 static cases (figs. 3 to 15), errors in displacements between MHOST-MARC and MHOST-MSC/NASTRAN are typically under 3.0 percent. The errors in stress and stress resultant predictions also happen to be generally under 3.0 percent, while moment resultant predictions increase slightly between MHOST-MARC to under 4.0 percent and increase by an order of magnitude between MHOST-MSC/NASTRAN to under 13.0 percent for most cases. As noted previously, similarities in the displacement based formulation of MHOST and MARC account for the smaller errors between these two codes.

The larger differences between MHOST and MSC/NASTRAN for stress and moment predictions can be attributed to two factors. The first factor is the differences in the formulation of the two codes, as noted above. The second factor arises due to the evaluation of forces and stresses at different points in the element by MHOST and MSC/NASTRAN. For the plate element, forces and stresses are extracted at the nodes by MHOST and at the center of the element by MSC/NASTRAN. In problems involving a uniform loading of the plate, the difference in the extraction points has a minimal effect. However, when a concentrated force is applied, this effect is no longer negligible in the region of the force. Typically, the problems which have a larger difference in stresses and moments between MHOST and MSC/NASTRAN contain a concentrated force.

Two additional static analysis cases for a rectangular plate (table IV) are included to gauge the effects of larger aspect ratios on the comparisons between the three codes. The dimensions of the rectangular plate are 20 in. long, 5 in. wide, and 0.2 in. thick. The finite element model for the rectangular plate consists of 400 isoparametric membrane-bending elements to maintain a 1:1 aspect ratio for each element. Both cases involve a distributed pressure load on a simply supported plate. The first problem (fig. 22) makes use of isotropic properties, while the second problem contains anisotropic properties. Comparisons of displacements and stresses for the isotropic case indicates similarly good agreement as found in the square plate (fig. 4). The anisotropic case for the rectangular plate shows slightly larger differences between for displacements and the moment resultant around the x-axis from the square plate (fig. 10). However, since the larger differences occur only for the anisotropic case, conclusions regarding the effect of aspect ratio, as well as the effect of different material properties, cannot be made without studying more cases.

In the free vibration analysis, MSC/NASTRAN predictions for the first three natural frequencies are conservative of their respective MHOST and MARC values. This is an expected consequence due to the use of the default lumped mass matrix in MSC/NASTRAN instead of the consistent mass matrix which is employed by MHOST and MARC. The different mass

matrices employed also accounts for the larger differences obtained between MHOST and MSC/NASTRAN results for the free vibration analysis.

The good agreement between the three codes in displacement predictions lends confidence to the use of MHOST for the various analyses in this study. This confidence in MHOST is further reinforced by the overall agreement between predictions of stresses, stress resultants, and moment resultants in the static analysis, the predictions of critical buckling load in the buckling analysis, and the determination of the first three natural frequencies in the free vibration analysis.

CONCLUSIONS

Good agreement is found between MHOST-MARC and MHOST-MSC/NASTRAN results for the static, buckling, and free vibration analyses of a plate element. In the static analysis, differences of less than 3.0 percent exists between the three codes for predictions of displacements. A difference of less than 6.0 percent is found for both the predictions of the critical buckling load and the first three natural frequencies, in the buckling and vibration analyses, respectively. The results of the evaluation indicate that MHOST can be used effectively and with confidence to perform static, buckling, and free vibration analyses using the plate element.

REFERENCES

1. Nakazawa, S.: The MHOST Finite Element Program: 3-D Inelastic Analysis Methods for Hot Section Components. Volume II-User's Manual. NASA CR-182235-VOL-2, 1989.
2. Chamis, C.C.; and Smith, G.T.: CODSTRAN: Computational Durability Structural Analysis. NASA TM-79070, 1978.
3. Singhal, S.N.; Lackney, J.J.; and Chamis, C.C.: Demonstration of Capabilities of High Temperature Composite Analyzer Code HITCAN. NASA TM-102560, 1990.
4. Narayanan, G.V., et al.: STAHYC User Manual, Version 1.0, 1991. Sverdrup Technology, Inc., Cleveland, OH.
5. MSC/NASTRAN, Version 65C, User's Manual. The MacNeal-Schwendler Corporation, Los Angeles, CA, 1987.
6. MARC, User Information Manual. MARC Analysis Research Corporation, 1988.

TABLE I.—PLATE ELEMENT, LINEAR ELASTIC STATIC ANALYSIS

Problem number	Geometry	Boundary conditions	Loading	Material	Agreement within	MHOST versus MARC or theory, percent	MHOST versus MSC/ NASTRAN, percent
1	Square plate	All edges simply supported	Concentrated load	Isotropic	For displacements	1.2	1.6
					For stresses	0.1	13.4
2	Square plate	All edges simply supported	Distributed load	Isotropic	For displacement	0.7	0.1
					For stresses	0.1	2.9
3	Square plate	All edges pinned (displacements not allowed, rotations allowed)	Uniform heating	Isotropic	For displacement	0	0
					For stresses	0	0
4	Square plate	All edges restrained to prevent rotations (middle plane free to expand)	Temperature gradient through the thickness	Isotropic	For displacement	0	0
					For stresses	0	0
5	Square plate	Edges restrained for normal displacements and rotations	Distributions load + uniform heating	Isotropic	For displacement	2.2	0
					For stresses	0.2	0.1
6	Square plate	All edges restrained to prevent rotations (middle plane free to expand)	Edge load + temperature gradient through the thickness	Isotropic	For displacement	0	0
					For stresses	0	1.6
7	Square plate	Three edges simply supported one edge free	Concentrated load	Anisotropic	For displacements	0.9	1.2
					For stress/moment resultants	2.3	13.1
8	Square plate	All edges simply supported	Distributed loads	Anisotropic	For displacements	0.2	0.3
					For stress/moment resultants	0	4.8
9	Square plate	All edges restrained to prevent rotations (middle plane free to expand)	Uniform heating	Anisotropic	For displacements	0	0
					For stress/moment resultants	0.1	0.1
10	Square plate	Three edges simply supported one edge free	Temperature gradient through the thickness	Anisotropic	For displacements	0	0.2
					For stress/moment resultants	3.2	13
11	Square plate	Three edges simply supported one edge free	Concentrated load + uniform heating	Anisotropic	For displacements	0.9	1.2
					For stress/moment resultants	2.3	12.7
12	Square plate	Three edges simply supported one edge free	Concentrated load + temperature gradient through the thickness	Anisotropic	For displacements	0.1	0.1
					For stress/moment resultants	1.6	4.4

TABLE II.—PLATE ELEMENT, LINEAR ELASTIC BUCKLING ANALYSIS

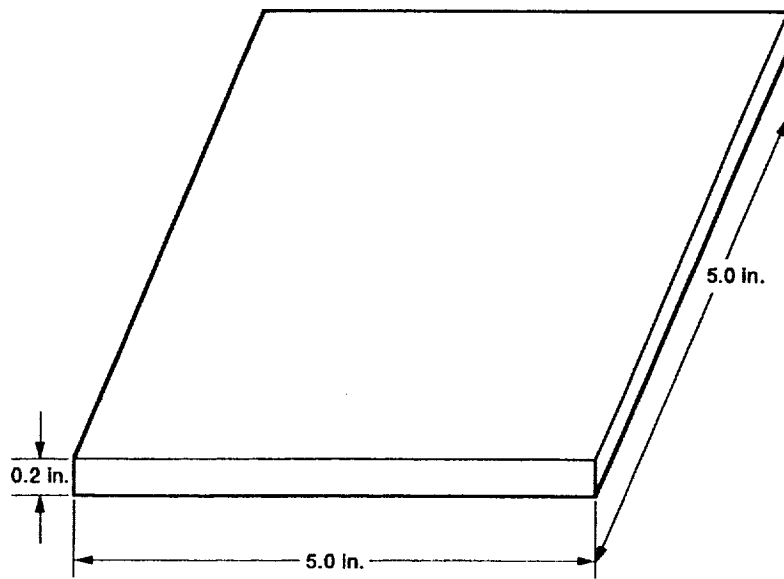
Problem number	Geometry	Boundary conditions	Loading	Material	Agreement for critical buckling load within	
					MHOST versus MARC, percent	MHOST versus MSC/NASTRAN, percent
13	Square plate	Two edges simply supported two Edges fixed	Compressive edge load	Isotropic	2.2	1.2
14	Square plate	Two edges simply supported two Edges fixed	Compressive edge + load + uniform heating	Isotropic	3.2	5.7
15	Square plate	All edges simply supported	Compressive edge load	Anisotropic	2.2	2.9

TABLE III.— PLATE ELEMENT, LINEAR ELASTIC FREE VIBRATION ANALYSIS

Problem number	Geometry	Boundary conditions	Loading	Material	Agreement for critical buckling load within		
					Mode	MHOST versus MARC, percent	MHOST versus MSC/NASTRAN, percent
16	Square plate	All edges clamped	-----	Isotropic	1	0.3	1.9
					2	0.6	4.8
					3	1.2	4.4
17	Square plate	Two edges simply supported two edges fixed	-----	Isotropic	1	0.3	1.9
					2	0.6	3.5
					3	0.5	5.2
18	Square plate	All edges clamped	-----	Anisotropic	1	0.3	0.06
					2	0.6	2.9
					3	0.6	2.3
19	Square plate	Two edges simply supported two edges fixed	-----	Anisotropic	1	0.3	0.2
					2	0.6	1.7
					3	0.5	3.5

TABLE IV.--PLATE ELEMENT, LINEAR ELASTIC STATIC ANALYSIS

Problem number	Geometry	Boundary conditions	Loading	Material	Agreement within	MHOST versus MARC, percent	MHOST versus MSC/NASTRAN, percent
20	Rectangular plate	All edges simply supported	Distributed load	Isotropic	For displacements	0.7	1.1
					For stresses	0.8	1.0
21	Rectangular plate	All edges simply supported	Distributed load	Anisotropic	For displacements	3.6	3.6
					For stress/moment resultants	14.7	14.0



(a) Schematic of plate model.

111	112	113	114	115	116	117	118	119	120	121
100	101	102	103	104	105	106	107	108	109	110
89	90	91	92	93	94	95	96	97	98	99
78	79	80	81	82	83	84	85	86	87	88
67	68	69	70	71	72	73	74	75	76	77
56	57	58	59	60	61	62	63	64	65	66
45	46	47	48	49	50	51	52	53	54	55
34	35	36	37	38	39	40	41	42	43	44
23	24	25	26	27	28	29	30	31	32	33
12	13	14	15	16	17	18	19	20	21	22
1	2	3	4	5	6	7	8	9	10	11

(b) Finite element mesh showing node numbers.

91	92	93	94	95	96	97	98	99	100
81	82	83	84	85	86	87	88	89	90
71	72	73	74	75	76	77	78	79	80
61	62	63	64	65	66	67	68	69	70
51	52	53	54	55	56	57	58	59	60
41	42	43	44	45	46	47	48	49	50
31	32	33	34	35	36	37	38	39	40
21	22	23	24	25	26	27	28	29	30
11	12	13	14	15	16	17	18	19	20
1	2	3	4	5	6	7	8	9	10

(c) Finite element mesh showing element numbers.

Figure 1.—

Isotropic material properties

Modulus of elasticity, $E = 10 \times 10^6$ psi
 Coefficient of thermal expansion, $\alpha = 1.3 \times 10^{-6}/^\circ\text{F}$
 Poisson's ratio, $\nu = 0.3$
 Density, $\rho = 0.000284$ lbm/in.³

Anisotropic material properties
 (SIC/11-15-3-3-3)

$E_{xx} = 36\,421\,401$ psi $\nu_{xy} = 0.264$
 $E_{yy} = 25\,653\,132$ psi $\nu_{yz} = 0.329$
 $E_{zz} = 23\,828\,149$ psi $\nu_{zy} = 0.320$
 $G_{xy} = 8\,985\,000$ psi $\alpha_{xx} = 2.73 \times 10^{-6}/^\circ\text{F}$
 $G_{yz} = 8\,917\,747$ psi $\alpha_{yy} = 2.84 \times 10^{-6}/^\circ\text{F}$
 $G_{zx} = 8\,959\,911$ psi $\alpha_{zz} = 2.84 \times 10^{-6}/^\circ\text{F}$
 Density, $\rho = 3.65 \times 10^{-4}$ lbm/in.³

Ply lay-up in z-direction

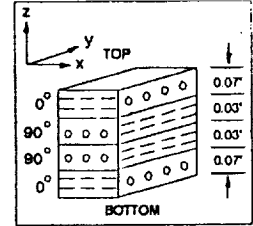
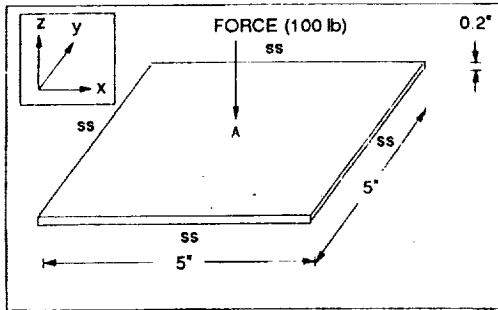


Figure 2.—Isotropic and anisotropic material properties.

Geometry, Boundary Conditions, and Loading



Material Properties

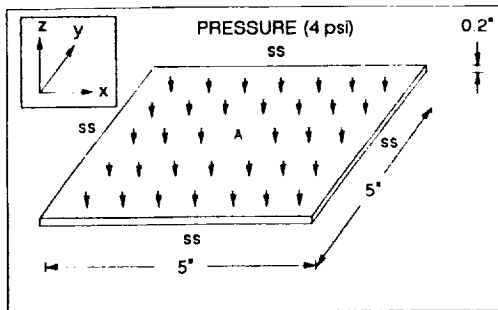
Modulus of elasticity, $E = 10 \times 10^6$ psi
 Coefficient of thermal expansion, $\alpha = 1.3 \times 10^{-6}/^\circ\text{F}$
 Poisson's ratio, $\nu = 0.3$
 Density, $\rho = 0.000284$ lbm/in.³

Displacement and Stress Results

Result \ Source	MHOST	MARC	MSC/ NASTRAN	% Difference MHOST vs.	
				MARC	MSC/ NASTRAN
Displacement in z-direction at center of midplane (inch)	-0.004074	-0.004024	-0.004009	1.2	1.6
Stress at top center, A (psi)					
in x-direction	3690.0	-3005.0	3252.4	0.1	13.4
in y-direction	-3690.0	-3695.0	-3252.4	0.1	13.4

Figure 3.—Problem #1: Square plate, all edges simply supported, concentrated load at top center, isotropic material, linear elastic constitutive model.

Geometry, Boundary Conditions, and Loading



Material Properties

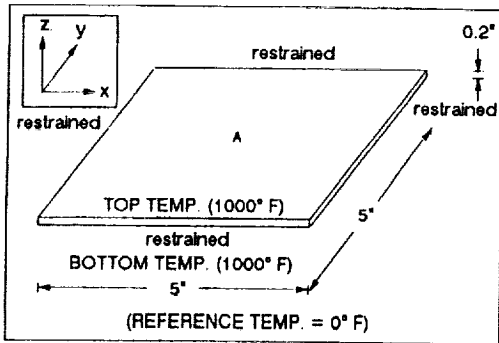
Modulus of elasticity, $E = 10 \times 10^6$ psi
 Coefficient of thermal expansion, $\alpha = 1.3 \times 10^{-6}/^\circ\text{F}$
 Poisson's ratio, $\nu = 0.3$
 Density, $\rho = 0.000284$ lbm/in.³

Displacement and Stress Results

Result \ Source	MHOST	Theory	MSC/ NASTRAN	% Difference MHOST vs.	
				Theory	MSC/ NASTRAN
Displacement in z-direction at center of midplane (inch)	0.001393	-0.001384	-0.001392	0.7	0.1
Stress at top center, A (psi)					
in x-direction	719.5	-718.5	698.9	0.1	2.9
in y-direction	719.5	-718.5	698.7	0.1	2.0

Figure 4.—Problem #2: Square plate, all edges simply supported, distributed load at top surface, isotropic material, linear elastic constitutive model. (Reference: "Theory and Analysis of Plates" by R. Szilard, 1974, p. 650).

Geometry, Boundary Conditions, and Loading



Material Properties

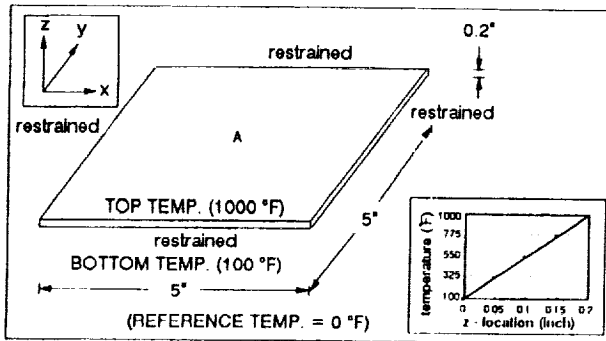
Modulus of elasticity, $E = 10 \times 10^6$ psi
 Coefficient of thermal expansion, $\alpha = 1.3 \times 10^{-6}$ /°F
 Poisson's ratio, $\nu = 0.3$
 Density, $\rho = 0.000284$ lbm/in³

Displacement and Stress Results

Result \ Source	MHOST	Theory	MSC/NASTRAN	% Difference MHOST vs.	
				Theory	MSC/NASTRAN
Displacement in z-direction at center of midplane (inch)	~0	~0	~0	~0	~0
Stress at top center, A (psi)					
	in x-direction	-18571.0	-18571.4	-18571.4	~0
in y-direction	-18571.0	-18571.4	-18571.4	~0	~0

Figure 5.—Problem #3: Square plate, all edges restrained (displacements not allowed, rotations allowed) uniform heating, isotropic material, linear elastic constitutive model. (Reference: "Theory of Thermal Stresses" by B. A. Boley and J. H. Weiner, 1960, p. 396).

Geometry, Boundary Conditions, and Loading



Material Properties

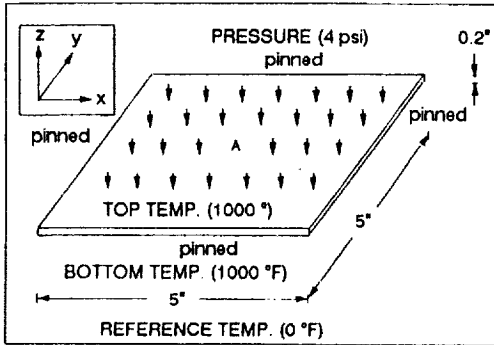
Modulus of elasticity, $E = 10 \times 10^6$ psi
 Coefficient of thermal expansion, $\alpha = 1.3 \times 10^{-6}$ /°F
 Poisson's ratio, $\nu = 0.3$
 Density, $\rho = 0.000284$ lbm/in³

Displacement and Stress Results

Result \ Source	MHOST	MARC	MSC/NASTRAN	% Difference MHOST vs.	
				MARC	MSC/NASTRAN
Displacement in z-direction at center of midplane (inch)	~0	~0	~0	~0	~0
Stress at top center, A (psi)					
	in x-direction	8357.1	8357.1	8357.1	0
in y-direction	8357.1	8357.1	8357.1	0	0

Figure 6.—Problem #4: Square plate, all edges restrained to prevent rotations (middle plane free to expand), nonuniform heating through thickness in z-direction, isotropic material, linear elastic constitutive model.

Geometry, Boundary Conditions, and Loading



Material Properties

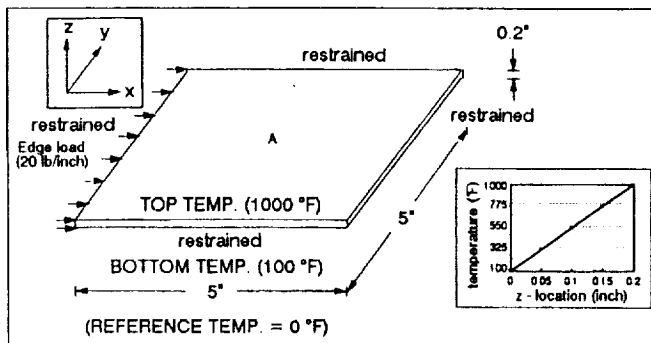
Modulus of elasticity, $E = 10 \times 10^6$ psi
 Coefficient of thermal expansion, $\alpha = 1.3 \times 10^{-6}$ /°F
 Poisson's ratio, $\nu = 0.3$
 Density, $\rho = 0.000284$ lbm/in³

Displacement and Stress Results

Result \ Source	Source			% Difference	
	MHOIST	MAVIC	MSC/NASTRAN	MHOIST vs. MAVIC	MHOIST vs. MSC/NASTRAN
Displacement in z-direction at center of midplane (inch)	-0.00044	-0.00043	-0.00044	2.2	0
Stress at top center, A (psi)					
in x-direction	-18921.0	-18950.5	-18903.6	0.2	0.1
in y-direction	-18921.0	-18950.5	-18903.6	0.2	0.1

Figure 7.—Problem #5: Square plate, edges restrained for normal displacement, and rotations, distributed load at top surface + uniform heating, isotropic material, linear constitutive model.

Geometry, Boundary Conditions, and Loading



Material Properties

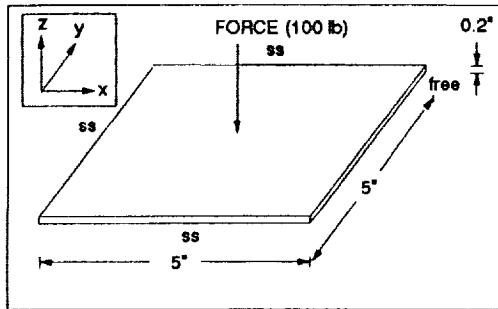
Modulus of elasticity, $E = 10 \times 10^6$ psi
 Coefficient of thermal expansion, $\alpha = 1.3 \times 10^{-6}$ /°F
 Poisson's ratio, $\nu = 0.3$
 Density, $\rho = 0.000284$ lbm/in³

Displacement and Stress Results

Result \ Source	Source			% Difference	
	MHOIST	Theory	MSC/NASTRAN	MHOIST vs. MAVIC	MHOIST vs. MSC/NASTRAN
Displacement in z-direction at center of midplane (inch)	~0	~0	~0	~0	~0
Stress at top center, A (psi)					
in x-direction	8257.1	8257.1	8388.1	0	1.6
in y-direction	8257.1	8257.1	8322.0	0	0.8

Figure 8.—Problem #6: Square plate, all edges restrained to prevent rotations (middle plane free to expand), edge load at left edge + nonuniform heating through thickness in z-direction, isotropic material, linear elastic constitutive model.

Geometry, Boundary Conditions, and Loading

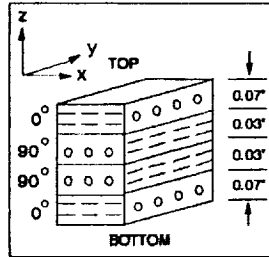


Material Properties

(SiC/Ti-15-3-3-3)

$E_{xx} = 36,421,401 \text{ psi}$	$\nu_{xy} = 0.264$
$E_{yy} = 25,653,132 \text{ psi}$	$\nu_{yz} = 0.329$
$E_{zz} = 23,828,149 \text{ psi}$	$\nu_{zy} = 0.320$
$G_{xz} = 8,985,000 \text{ psi}$	$\alpha_{xx} = 2.73 \times 10^{-6} / ^\circ\text{F}$
$G_{xy} = 8,917,747 \text{ psi}$	$\alpha_{yy} = 2.84 \times 10^{-6} / ^\circ\text{F}$
$G_{yz} = 8,959,911 \text{ psi}$	$\alpha_{zz} = 2.84 \times 10^{-6} / ^\circ\text{F}$
Density, $\rho = 3.65 \times 10^{-4} \text{ lbm/in}^3$	

Ply lay-up in z-direction

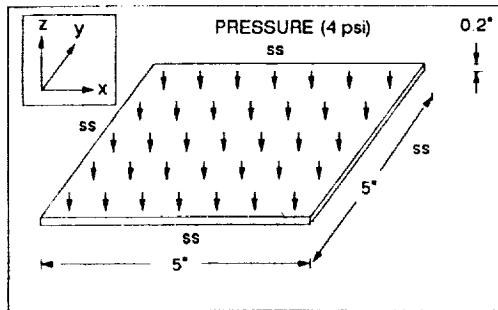


Displacement and Stress Results

Source Result	MI/OST	MARC	MSC/ NASTRAN	% Difference MI/OST vs.	
				MARC	MSC/ NASTRAN
Displacement in z-direction at center of midplane (inchi)	-0.002289	-0.002268	-0.002261	0.9	1.2
Stress resultant at center plane (lb/in)					
in x-direction	~0	~0	~0	~0	~0
in y-direction	~0	~0	~0	~0	~0
Moment resultant at center plane (lb-in/in)					
in x-direction	-25.8	-26.4	-22.8	2.3	13.1
in y-direction	-26.9	-27.0	-24.3	0.4	10.5

Figure 9.—Problem #7: Square plate, 3 edges simply supported and 1 edge free, concentrated load at top center, anisotropic 4-layered (0/90)_s composite metal matrix material SiC/Ti-15-3-3-3, linear elastic constitutive model.

Geometry, Boundary Conditions, and Loading

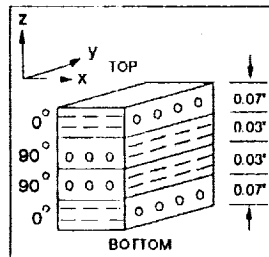


Material Properties

(SiC/Ti-15-3-3-3)

$E_{xx} = 36,421,401 \text{ psi}$	$\nu_{xy} = 0.264$
$E_{yy} = 25,653,132 \text{ psi}$	$\nu_{yz} = 0.329$
$E_{zz} = 23,828,149 \text{ psi}$	$\nu_{zy} = 0.320$
$G_{xz} = 8,985,000 \text{ psi}$	$\alpha_{xx} = 2.73 \times 10^{-6} / ^\circ\text{F}$
$G_{xy} = 8,917,747 \text{ psi}$	$\alpha_{yy} = 2.84 \times 10^{-6} / ^\circ\text{F}$
$G_{yz} = 8,959,911 \text{ psi}$	$\alpha_{zz} = 2.84 \times 10^{-6} / ^\circ\text{F}$
Density, $\rho = 3.65 \times 10^{-4} \text{ lbm/in}^3$	

Ply lay-up in z-direction

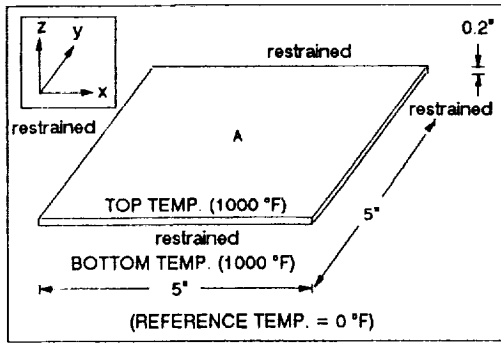


Displacement and Stress Results

Source Result	MI/OST	MARC	MSC/ NASTRAN	% Difference MI/OST vs.	
				MARC	MSC/ NASTRAN
Displacement in z-direction at center of midplane (inchi)	-0.000532	-0.000531	-0.000529	0.2	0.3
Stress resultant at midplane (lb/in)					
in x-direction	~0	~0	~0	~0	~0
in y-direction	~0	~0	~0	~0	~0
Moment resultant at midplane (lb-in/in)					
in x-direction	-5.9	-5.9	-5.7	0	3.5
in y-direction	-4.4	-4.4	-4.2	0	4.8

Figure 10.—Problem #8: Square plate, all edges simply supported, distributed load surface anisotropic 4-layered (0/90)_s composite metal matrix material SiC/Ti-15-3-3-3, linear elastic constitutive model.

Geometry, Boundary Conditions, and Loading

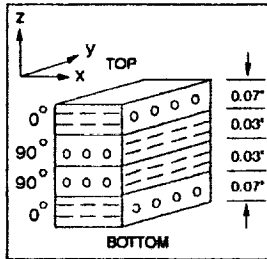


Material Properties

(SiC/Ti-15-3-3-3)

$E_{xx} = 36,421,401$ psi,	$\nu_{xy} = 0.264$
$E_{yy} = 25,653,132$ psi,	$\nu_{yz} = 0.320$
$E_{zz} = 23,828,149$ psi,	$\nu_{zy} = 0.320$
$G_{xy} = 8,985,000$ psi,	$\alpha_{xx} = 2.73 \times 10^{-6}$ /°F
$G_{yz} = 8,917,747$ psi,	$\alpha_{yy} = 2.84 \times 10^{-6}$ /°F
$G_{zx} = 8,959,911$ psi,	$\alpha_{zz} = 2.84 \times 10^{-6}$ /°F
Density, $\rho = 3.65 \times 10^{-4}$ lbm/in ³	

Ply lay-up in z-direction

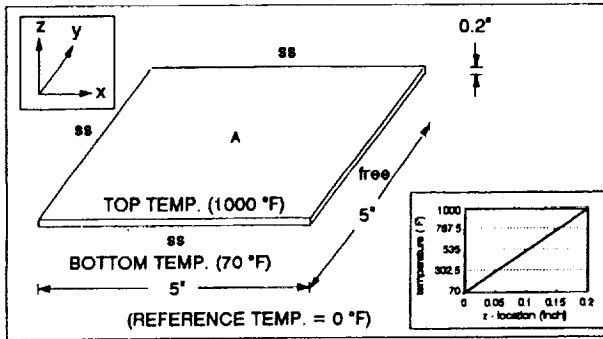


Displacement and Stress Results

Result \ Source	MH-OST	MARC	MSC/ NASTRAN	% Difference MH-OST vs.	
				MARC	MSC/ NASTRAN
Displacement in z-direction at center of midplane (inch)	~0	~0	~0	~0	~0
Stress resultant at center plane (lb/in)					
in x-direction	-24945.0	-24960.0	-24958.2	0.1	0.1
in y-direction	-19213.0	-19212.0	-19211.8	~0	~0
Moment resultant at center plane (lb-in/in)					
in x-direction	~0	~0	~0	0	0
in y-direction	~0	~0	~0	0	0

Figure 11.—Problem #9: Square plate, all edges restrained to prevent rotations (middle plane free to expand), uniform heating, anisotropic 4-layered (0/90)_s composite metal matrix material SiC/Ti-15-3-3-3, linear elastic constitutive model.

Geometry, Boundary Conditions, and Loading

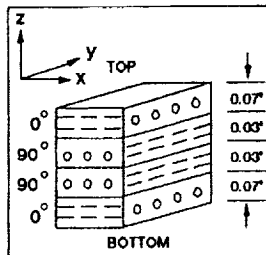


Material Properties

(SiC/Ti-15-3-3-3)

$E_{xx} = 36,421,401$ psi,	$\nu_{xy} = 0.264$
$E_{yy} = 25,653,132$ psi,	$\nu_{yz} = 0.320$
$E_{zz} = 23,828,149$ psi,	$\nu_{zy} = 0.320$
$G_{xy} = 8,985,000$ psi,	$\alpha_{xx} = 2.73 \times 10^{-6}$ /°F
$G_{yz} = 8,917,747$ psi,	$\alpha_{yy} = 2.84 \times 10^{-6}$ /°F
$G_{zx} = 8,959,911$ psi,	$\alpha_{zz} = 2.84 \times 10^{-6}$ /°F
Density, $\rho = 3.65 \times 10^{-4}$ lbm/in ³	

Ply lay-up in z-direction

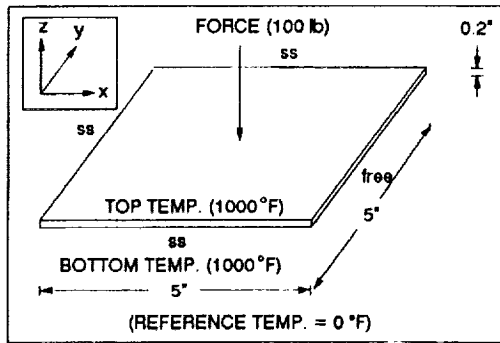


Displacement and Stress Results

Result \ Source	MH-OST	MARC	MSC/ NASTRAN	% Difference MH-OST vs.	
				MARC	MSC/ NASTRAN
Displacement in z-direction at center of midplane (inch)	0.04216	0.04216	0.04205	0	0.2
Stress resultant at midplane (lb/in)					
in x-direction	~0	~0	~0	~0	~0
in y-direction	-7805.0	-7798.0	-7798.0	0.1	0.1
Moment resultant at midplane (lb-in/in)					
in x-direction	-119.7	-118.3	-128.4	1.2	7.5
in y-direction	-31.9	-30.9	-36.7	3.2	13.0

Figure 12.—Problem #10: Square plate, 3 edges simply supported and 1 edge free, nonuniform heating through thickness in z-direction, anisotropic 4-layered (0/90)_s composite metal matrix material SiC/Ti-15-3-3-3, linear elastic constitutive model.

Geometry, Boundary Conditions, and Loading

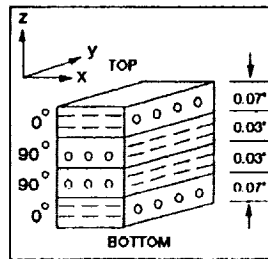


Material Properties

(SiC/Ti-15-3-3-3)

$E_{xx} = 36,421,401$ psi,	$\nu_{xy} = 0.264$
$E_{yy} = 25,653,132$ psi,	$\nu_{yz} = 0.320$
$E_{zz} = 23,828,149$ psi,	$\nu_{zy} = 0.320$
$G_{xy} = 8,985,000$ psi,	$\alpha_{xx} = 2.73 \times 10^{-6}/^{\circ}\text{F}$
$G_{yz} = 8,917,747$ psi,	$\alpha_{yy} = 2.84 \times 10^{-6}/^{\circ}\text{F}$
$G_{zx} = 8,959,911$ psi,	$\alpha_{zz} = 2.84 \times 10^{-6}/^{\circ}\text{F}$
Density, $\rho = 3.65 \times 10^{-4}$ lbm/in ³	

Ply lay-up in z-direction

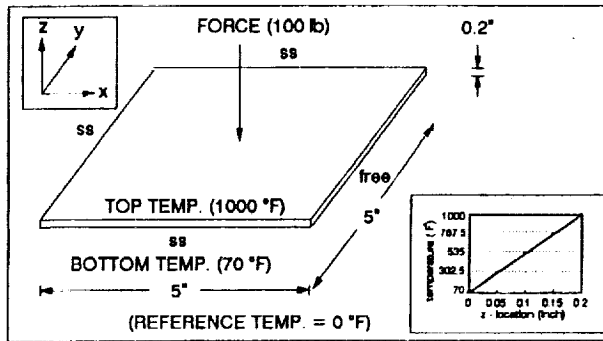


Displacement and Stress Results

Result \ Source	MHOST	MARC	MSC/ NASTRAN	% Difference MHOST vs.	
				MARC	MSC/NASTRAN
Displacement in z-direction at center of midplane (inch)	-0.002289	-0.002260	-0.002261	0.0	1.2
Stress resultant at center plane (lb/in)					
in x-direction	~0	~0	~0	~0	~0
in y-direction	-14588.0	-14570.0	-14570.0	0.12	0.12
Moment resultant at center plane (lb-in/in)					
in x-direction	-25.8	-26.4	-22.9	2.3	12.7
in y-direction	-26.9	-27.0	-24.4	0.4	10.5

Figure 13.—Problem #11: Square plate, 3 edges simply supported and 1 edge free, concentrated load + uniform heating, anisotropic 4-layered (0/90)_s composite metal matrix material SiC/Ti-15-3-3-3, linear elastic constitutive model.

Geometry, Boundary Conditions, and Loading

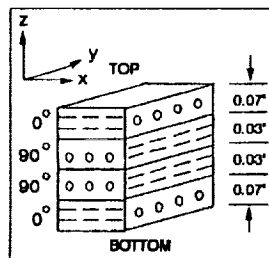


Material Properties

(SiC/Ti-15-3-3-3)

$E_{xx} = 36,421,401$ psi,	$\nu_{xy} = 0.264$
$E_{yy} = 25,653,132$ psi,	$\nu_{yz} = 0.320$
$E_{zz} = 23,828,149$ psi,	$\nu_{zy} = 0.320$
$G_{xy} = 8,985,000$ psi,	$\alpha_{xx} = 2.73 \times 10^{-6}/^{\circ}\text{F}$
$G_{yz} = 8,917,747$ psi,	$\alpha_{yy} = 2.84 \times 10^{-6}/^{\circ}\text{F}$
$G_{zx} = 8,959,911$ psi,	$\alpha_{zz} = 2.84 \times 10^{-6}/^{\circ}\text{F}$
Density, $\rho = 3.65 \times 10^{-4}$ lbm/in ³	

Ply lay-up in z-direction

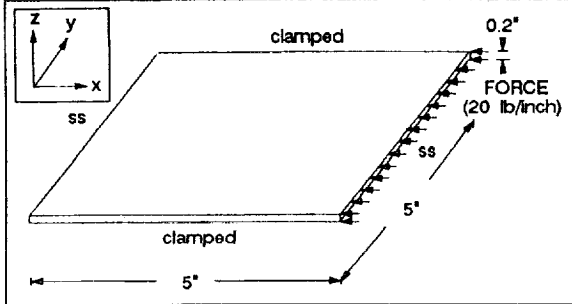


Displacement and Stress Results

Result \ Source	MHOST	MARC	MSC/ NASTRAN	% Difference MHOST vs.	
				MARC	MSC/NASTRAN
Displacement in z-direction at center of midplane (inch)	0.03987	0.03989	0.03982	0.1	0.1
Stress resultant at center plane (lb/in)					
in x-direction	~0	~0	~0	~0	~0
in y-direction	-7805.0	-7798.0	-7796.0	0.1	0.1
Moment resultant at center plane (lb-in/in)					
in x-direction	-145.5	-144.7	-152.2	0.6	4.4
in y-direction	-58.8	-57.9	-61.0	1.6	3.6

Figure 14.—Problem #12: Square plate, 3 edges simply supported and 1 edge free, concentrated load + nonuniform heating through thickness in z-direction, anisotropic 4-layered (0/90)_s composite metal matrix material SiC/Ti-15-3-3-3, linear elastic constitutive model.

Geometry, Boundary Conditions, and Loading



Material Properties

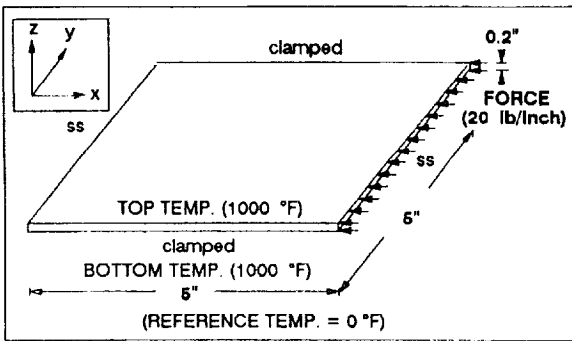
Modulus of elasticity, $E = 10 \times 10^6$ psi
 Coefficient of thermal expansion, $\alpha = 1.3 \times 10^{-6}$ /°F
 Poisson's ratio, $\nu = 0.3$
 Density, $\rho = 2.849 \times 10^{-4}$ lbm/in³

Critical Buckling Load Results

Result	Source	MHOST	MARC	MSC/ NASTRIAN	% Difference	
					MARC	MSC/ NASTRIAN
Critical Buckling Load (lb/inch)		25576.8	26140.0	25284.8	2.2	1.2

Figure 15.—Problem #13: Square plate, 2 edges simply supported and 2 edges clamped, compressive edge load, at right edge, isotropic material, linear elastic constitutive model.

Geometry, Boundary Conditions, and Loading



Material Properties

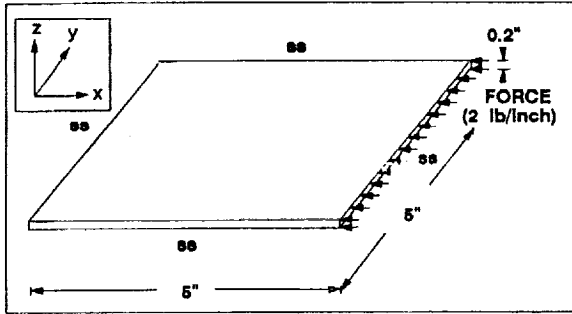
Modulus of elasticity, $E = 10 \times 10^6$ psi
 Coefficient of thermal expansion, $\alpha = 1.3 \times 10^{-6}$ /°F
 Poisson's ratio, $\nu = 0.3$
 Density, $\rho = 2.849 \times 10^{-4}$ lbm/in³

Critical Buckling Load Results

Result	Source	MHOST	MARC	MSC/ NASTRIAN	% Difference	
					MARC	MSC/ NASTRIAN
Critical Buckling Load (lb/inch)		89.6	86.8	84.5	3.2	5.7

Figure 16.—Problem #14: Square plate, 2 edges simply supported and 2 edges clamped, compressive edge load at right edge + uniform heating isotropic material, linear elastic constitutive model.

Geometry, Boundary Conditions, and Loading

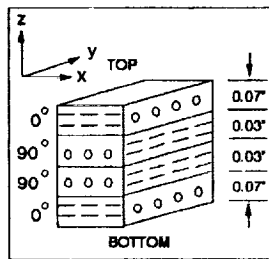


Material Properties

(SiC/Ti-15-3-3-3)

$E_{xx} = 36,421,401$ psi	$\nu_{xy} = 0.264$
$E_{yy} = 25,653,132$ psi	$\nu_{yz} = 0.329$
$E_{zz} = 23,828,149$ psi	$\nu_{zy} = 0.320$
$G_{xz} = 8,985,000$ psi	$\alpha_{xx} = 2.73 \times 10^{-6}/^{\circ}\text{F}$
$G_{xy} = 8,917,747$ psi	$\alpha_{yy} = 2.84 \times 10^{-6}/^{\circ}\text{F}$
$G_{yz} = 8,959,911$ psi	$\alpha_{zz} = 2.84 \times 10^{-6}/^{\circ}\text{F}$
Density, $\rho = 3.65 \times 10^{-4}$ lbm/in ³	

Ply lay-up in z-direction

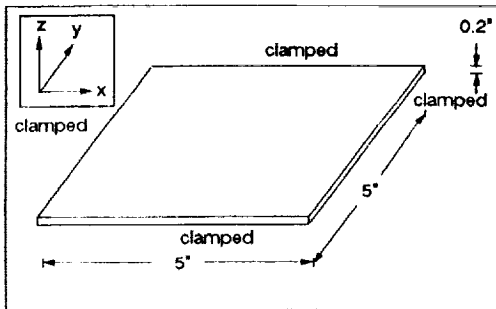


Critical Buckling Load Results

Result \ Source	MI-POST	MARC	MSC/ NASTRAN	% Difference	
				MARC	MSC/ NASTRAN
Critical Buckling Load (lb/inch)	31226.0	30440.0	30344.7	2.2	2.9

Figure 17.—Problem #15: Square plate, all edges simply supported, compressive edge load at right edge, anisotropic 4-layered (0/90)₀ composite metal matrix material SiC/Ti-15-3-3-3, linear constitutive model.

Geometry and Boundary Conditions



Natural Frequency Results

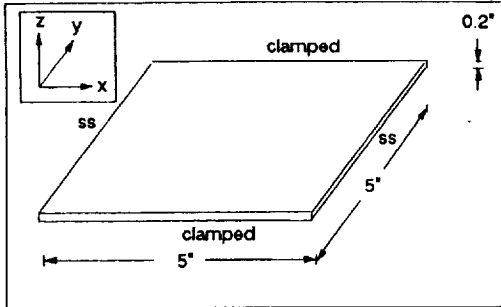
Result \ Source	MI-POST	MARC	MSC/ NASTRAN	% Difference	
				MARC	MSC/ NASTRAN
Mode 1 (cycles/sec)	2620.8	2629.5	2571.1	0.3	1.9
Mode 2	5501.8	5536.9	5252.5	0.8	4.8
Mode 3	8003.7	8103.5	7664.0	1.2	4.4

Material Properties

Modulus of elasticity, $E = 10 \times 10^6$ psi
Coefficient of thermal expansion, $\alpha = 1.3 \times 10^{-6}/^{\circ}\text{F}$
Poisson's ratio, $\nu = 0.3$
Density, $\rho = 0.000284$ lbm/in ³

Figure 18.—Problem #16: Square plate, all edges clamped, free vibration, isotropic material, linear constitutive model.

Geometry and Boundary Conditions



Natural Frequency Results

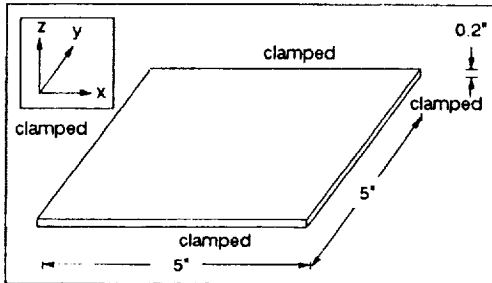
Result \ Source (cycles/sec)	MHOST	MARC	MSC/ NASTRAN	% Difference	
				MHOST vs. MARC	MHOST vs. MSC/NASTRAN
Mode 1	2102.20	2114.9	2070.4	0.3	1.9
Mode 2	4028.60	4052.0	3893.2	0.6	3.5
Mode 3	5233.1	5261.5	4975.7	0.5	5.2

Material Properties

Modulus of elasticity, $E = 10 \times 10^6$ psi
 Coefficient of thermal expansion, $\alpha = 1.3 \times 10^{-6}$ /°F
 Poisson's ratio, $\nu = 0.3$
 Density, $\rho = 0.000284$ lbm/in³

Figure 19.—Problem #17: Square plate, 2 edges simply supported and 2 edges clamped, free vibration, isotropic material, linear elastic constitutive model.

Geometry and Boundary Conditions



Natural Frequency Results

Result \ Source (cycles/sec)	MHOST	MARC	MSC/ NASTRAN	% Difference	
				MHOST vs. MARC	MHOST vs. MSC/NASTRAN
Mode 1	24363.0	24445.2	24349.1	0.3	0.06
Mode 2	48353.0	48645.0	48004.8	0.6	2.9
Mode 3	53802.0	54238.5	52692.1	0.6	2.3

Material Properties

(SiC/Ti-15-3-3-3)

$E_{xx} = 36,421,401$ psi, $\nu_{xy} = 0.264$
 $E_{yy} = 25,653,132$ psi, $\nu_{yz} = 0.329$
 $E_{zz} = 23,828,149$ psi, $\nu_{zy} = 0.320$
 $G_{xy} = 8,965,000$ psi, $\alpha_{xx} = 2.73 \times 10^{-6}$ /°F
 $G_{yz} = 8,917,747$ psi, $\alpha_{yy} = 2.84 \times 10^{-6}$ /°F
 $G_{zx} = 8,959,011$ psi, $\alpha_{zz} = 2.84 \times 10^{-6}$ /°F
 Density, $\rho = 3.65 \times 10^{-4}$ lbm/in³

Ply lay-up in z-direction

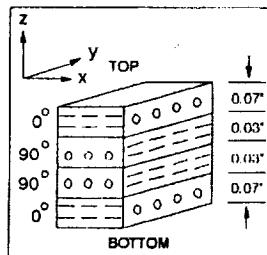
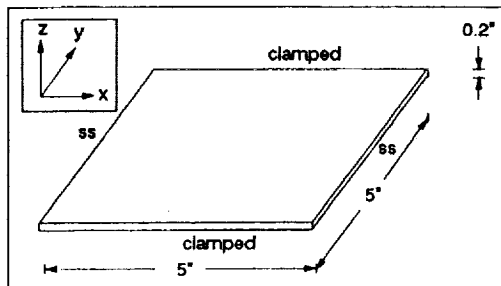


Figure 20.—Problem #18: Square plate, all edges clamped, free vibration, anisotropic 4-layered (0/90)₂ composite metal matrix material SiC/Ti-15-3-3-3, linear elastic constitutive model.

Geometry and Boundary Conditions

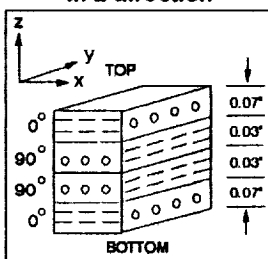


Material Properties

(SiC/Ti-15-3-3-3)

$E_{xx} = 36,421,401$ psi,	$\nu_{xy} = 0.264$
$E_{yy} = 25,653,132$ psi,	$\nu_{xy} = 0.329$
$E_{zz} = 23,828,149$ psi,	$\nu_{yz} = 0.320$
$G_{xy} = 8,985,000$ psi,	$\alpha_{xx} = 2.73 \times 10^{-6} / ^\circ F$
$G_{xy} = 8,917,747$ psi,	$\alpha_{yy} = 2.84 \times 10^{-6} / ^\circ F$
$G_{yz} = 8,959,911$ psi,	$\alpha_{zz} = 2.84 \times 10^{-6} / ^\circ F$
Density, $\rho = 3.65 \times 10^{-4}$ lbm/in ³	

Ply lay-up in z-direction

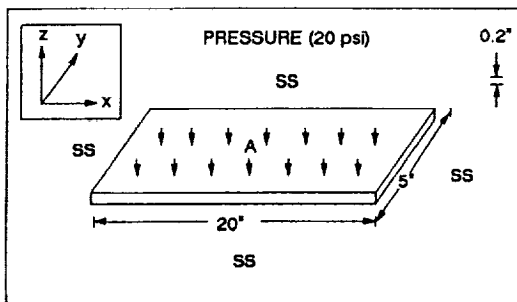


Natural Frequency Results

Result \ Source	MIHOST	MARC	MSC/NASTRAN	% Difference	
				MARC	MSC/NASTRAN
Mode 1	18594.0	18642.5	18552.6	0.3	0.2
Mode 2	38327.0	38550.4	37895.1	0.6	1.7
Mode 3	45365.0	45591.2	43850.7	0.5	3.5

Figure 21.—Problem #19: Square plate, 2 edges simply supported and 2 edges clamped, free vibration, anisotropic 4-layered (0/90)₂ composite metal matrix material SiC/Ti-15-3-3-3, linear elastic constitutive model.

Geometry, Boundary Conditions, and Loading



Material Properties

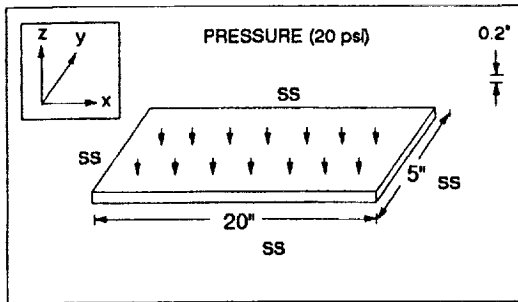
Modulus of elasticity, $E = 10 \times 10^6$ psi
Coefficient of thermal expansion, $\alpha = 1.3 \times 10^{-6} / ^\circ F$
Poisson's ratio, $\nu = 0.3$
Density, $\rho = 0.000284$ lbm/in ³

Displacement and Stress Results

Result \ Source	MIHOST	MARC	MSC/NASTRAN	% Difference	
				MIHOST vs. MARC	MIHOST vs. MSC/NASTRAN
Displacement in z-direction at center of midplane (inch)	-0.02146	-0.02182	-0.0217	0.7	1.1
Stress at top center, A (psi)					
in x-direction	-2848.0	-2824.0	-2821.0	0.8	1.0
in y-direction	-9028.0	-9083.0	-9078.0	0.6	0.6

Figure 22.—Problem #20: Rectangular plate, all edges simply supported, distributed load at surface, isotropic material, linear elastic constitutive model.

Geometry, Boundary Conditions, and Loading

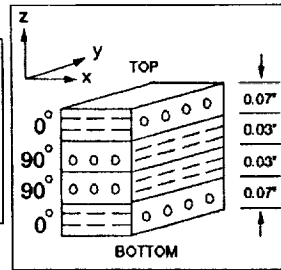


Material Properties

(SiC/Ti-15-3-3-3)

$E_{xx} = 36,421,401$ psi,	$\nu_{xy} = 0.284$
$E_{yy} = 25,653,132$ psi,	$\nu_{yz} = 0.329$
$E_{zz} = 23,828,149$ psi,	$\nu_{xy} = 0.320$
$G_{xy} = 8,985,000$ psi,	$\alpha_{xx} = 2.73 \times 10^{-6} / ^\circ F$
$G_{yz} = 8,917,747$ psi,	$\alpha_{yy} = 2.84 \times 10^{-6} / ^\circ F$
$G_{zx} = 8,959,911$ psi,	$\alpha_{zz} = 2.84 \times 10^{-6} / ^\circ F$
Density, $\rho = 3.85 \times 10^{-4} \text{ lb/in}^3$	

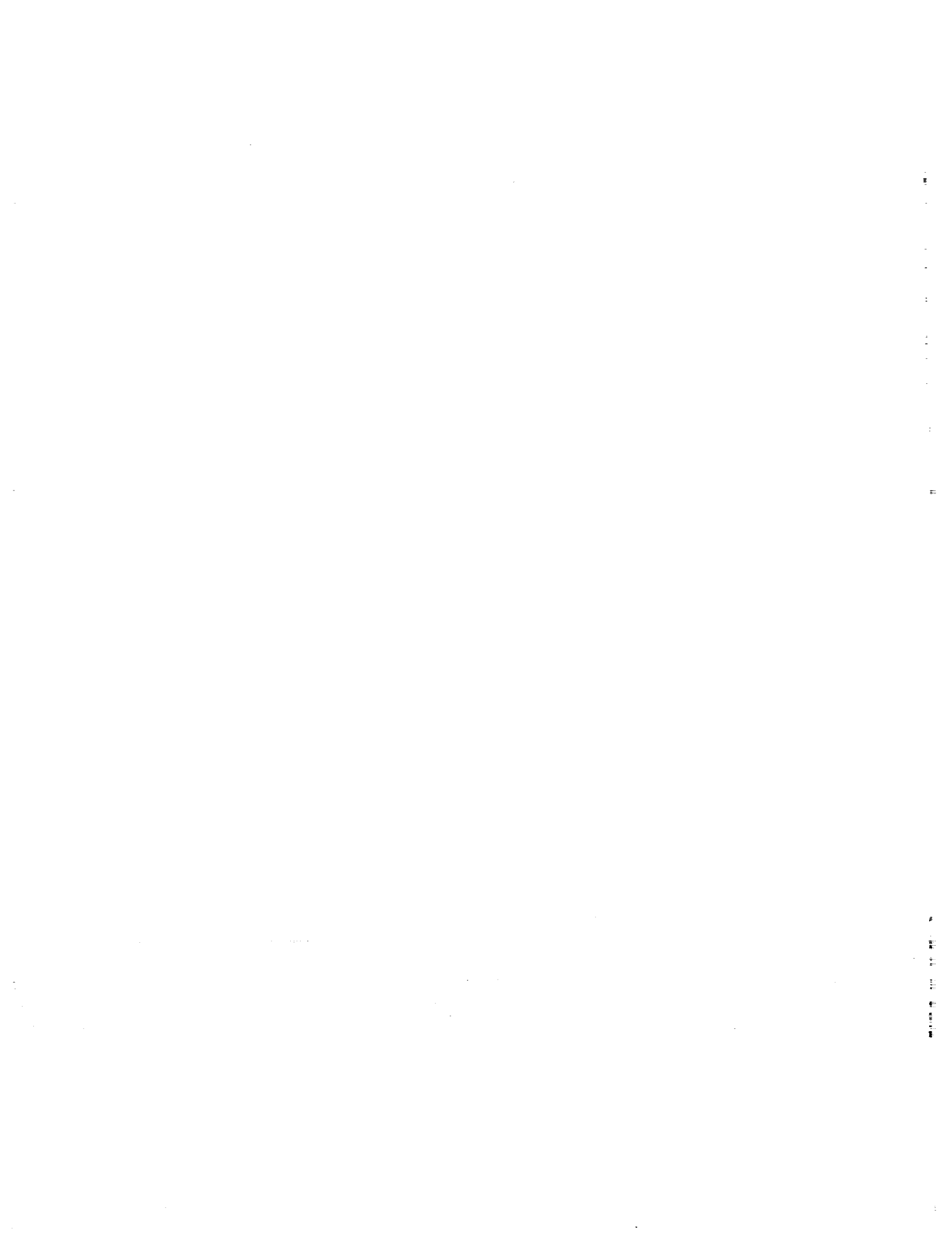
Ply lay-up in z-direction

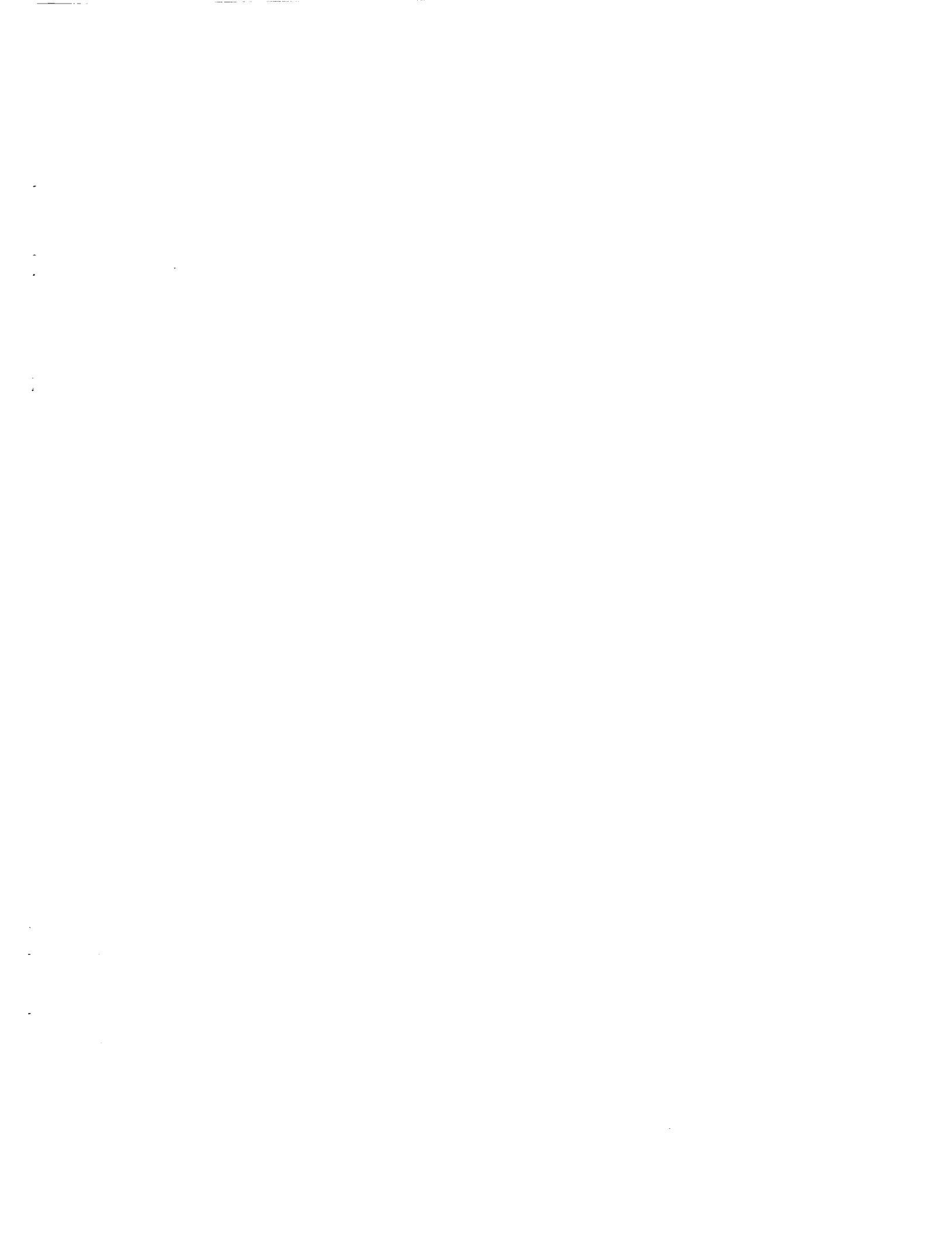


Displacement and Stress Results

Result	Source	MI-HOST	MARC	MSC/NASTRAN	% Difference	
					MARC	MSC/NASTRAN
Displacement in z-direction at center of midplane (inch)		-0.00922	-0.00890	-0.0089	3.6	3.6
Stress resultant at center plane (lb/in)						
in x-direction		~ 0	~ 0	~ 0	~ 0	~ 0
in y-direction		~ 0	~ 0	~ 0	~ 0	~ 0
Moment resultant at center plane (lb-in/in)						
in x-direction		-19.50	-17.0	-17.10	14.7	14.0
in y-direction		-60.42	-61.0	-61.0	0.9	0.9

Figure 23.—Problem #21: Rectangular plate, all edges simply supported, distributed load at surface, anisotropic 4-layered (0/90)_s composite metal matrix material SiC/Ti-15-3-3-3, linear elastic constitutive model.





REPORT DOCUMENTATION PAGE

Form Approved
OMB No. 0704-0188

Public reporting burden for this collection of information is estimated to average 1 hour per response, including the time for reviewing instructions, searching existing data sources, gathering and maintaining the data needed, and completing and reviewing the collection of information. Send comments regarding this burden estimate or any other aspect of this collection of information, including suggestions for reducing this burden, to Washington Headquarters Services, Directorate for Information Operations and Reports, 1215 Jefferson Davis Highway, Suite 1204, Arlington, VA 22202-4302, and to the Office of Management and Budget, Paperwork Reduction Project (0704-0188), Washington, DC 20503.

1. AGENCY USE ONLY (Leave blank)	2. REPORT DATE February 1992	3. REPORT TYPE AND DATES COVERED Technical Memorandum	
4. TITLE AND SUBTITLE Evaluation of MHOST Analysis Capabilities for a Plate Element		5. FUNDING NUMBERS WU-510-10-50	
6. AUTHOR(S) Ho-Jun Lee, Galib H. Abumeri, and Helen C. Brown			
7. PERFORMING ORGANIZATION NAME(S) AND ADDRESS(ES) National Aeronautics and Space Administration Lewis Research Center Cleveland, Ohio 44135-3191		8. PERFORMING ORGANIZATION REPORT NUMBER E-6773	
9. SPONSORING/MONITORING AGENCY NAMES(S) AND ADDRESS(ES) National Aeronautics and Space Administration Washington, D.C. 20546-0001		10. SPONSORING/MONITORING AGENCY REPORT NUMBER NASA TM-105387	
11. SUPPLEMENTARY NOTES Ho-Jun Lee, NASA Lewis Research Center; Galib H. Abumeri and Helen C. Brown, Sverdrup Technology, Inc., 2001 Aerospace Parkway, Brook Park, Ohio 44142. Responsible person, Ho-Jun Lee, (216) 433-3316.			
12a. DISTRIBUTION/AVAILABILITY STATEMENT Unclassified - Unlimited Subject Category 39		12b. DISTRIBUTION CODE	
13. ABSTRACT (Maximum 200 words) Results of the evaluation of the static, buckling, and free vibration analyses capabilities of MHOST for the plate element are presented. Two large scale, general purpose finite element codes (MARC and MSC/NASTRAN) are used to validate MHOST. Comparisons of MHOST results with those from MARC and MSC/NASTRAN show good agreement and indicate that MHOST can be used with confidence to perform the aforementioned analyses using the plate element.			
14. SUBJECT TERMS Anisotropic; Buckling; Comparison; Composite; Displacement; Finite element; Free vibration; Isotropic; Moment resultant; Plate element; Stress; Stress resultant; Static			15. NUMBER OF PAGES 22
			16. PRICE CODE A03
17. SECURITY CLASSIFICATION OF REPORT Unclassified	18. SECURITY CLASSIFICATION OF THIS PAGE Unclassified	19. SECURITY CLASSIFICATION OF ABSTRACT Unclassified	20. LIMITATION OF ABSTRACT